

Article

MSWI Fly Ash Multiple Washing: Kinetics of Dissolution in Water, as Function of Time, Temperature and Dilution

Caterina Caviglia ^{1,*} , Enrico Destefanis ¹ , Linda Pastero ¹ , Davide Bernasconi ¹ , Costanza Bonadiman ² and Alessandro Pavese ¹

¹ Dipartimento di Scienze della Terra, Università degli Studi di Torino, Via Valperga Caluso 35, 10125 Torino, Italy; enrico.destefanis@unito.it (E.D.); linda.pastero@unito.it (L.P.); davide.bernasconi@unito.it (D.B.); alessandro.pavese@unito.it (A.P.)

² Dipartimento di Fisica e Scienze della Vita, Università degli Studi di Ferrara, Via Saragat 1, 44122 Ferrara, Italy; costanza.bonadiman@unife.it

* Correspondence: caterina.caviglia@unito.it

Abstract: Municipal solid waste incineration fly ash (FA) can represent a sustainable supply of supplementary material to the construction industries if it is pre-treated to remove hazardous substances such as chloride, sulfate, and heavy metals. In this paper, the phenomenology associated with a water washing multi-cycle treatment of FA is investigated, focusing attention upon the mineral dissolution process. The efficacy of the treatment is assessed by leaching tests, according to the European Standard, and discussed in light of the occurring mineral phases. The water-to-solid (L/S) ratio is a crucial parameter, along with the number of washing cycles, for removing halite and sylvite, whereas quartz, calcite, anhydrite, and an amorphous phase remain in the solid residue. The sequential extraction method and dissolution kinetics modelling provide further elements to interpret leaching processes, and suggest that dissolution takes place through a two-step mechanism. Altogether, multi-step washing with L/S = 5 is effective in reducing contaminants under the legal limits for non-hazardous waste disposal, while the legal limits for non-reactive or reusable material cannot be completely reached, owing to sulfate and some heavy metals which still leached out from the residue.

Keywords: MSWI fly ash; multiple washing; kinetics of dissolution; mineralogy; reuse



Citation: Caviglia, C.; Destefanis, E.; Pastero, L.; Bernasconi, D.; Bonadiman, C.; Pavese, A. MSWI Fly Ash Multiple Washing: Kinetics of Dissolution in Water, as Function of Time, Temperature and Dilution. *Minerals* **2022**, *12*, 742. <https://doi.org/10.3390/min12060742>

Academic Editors: Mario Tribaudino and Alexander Mikhailovich Kalinkin

Received: 15 April 2022

Accepted: 8 June 2022

Published: 10 June 2022

Publisher's Note: MDPI stays neutral with regard to jurisdictional claims in published maps and institutional affiliations.



Copyright: © 2022 by the authors. Licensee MDPI, Basel, Switzerland. This article is an open access article distributed under the terms and conditions of the Creative Commons Attribution (CC BY) license (<https://creativecommons.org/licenses/by/4.0/>).

1. Introduction

Municipal solid waste incineration (MSWI) is, nowadays, a widespread technology for MSW disposal all over the world, allowing energy recovery and waste volume reduction of ~20–25 vol% [1,2]. Fly ash (FA) is a finely powdered waste that forms as a by-product in the flue gas purification system of MSWI and accounts for up to ~2–3% of the total waste [3,4]. MSWI-FA is classified as a hazardous waste by the European regulatory authorities [5] and contains CaO, SiO₂, SO₃, Fe₂O₃, Al₂O₃, and MgO as major oxides, commonly associated with water-leachable heavy metals (metal or metalloids with atomic number greater than 20, density above 5 g/cm³). The main mineralogical composition comprises several salts (in particular halide, sulfate, carbonate), along with a relevant amorphous fraction (up to 50 wt%) [6–12]. Because of these features, the recycling of MSWI-FA for profitable applications is challenging. For instance: the presence of carbonate salt and metal oxides leads to a highly basic natural pH (~10–12) [13–16]; the chloride content promotes corrosion of reinforced concrete structures [17]; the high water-absorption capacity of hygroscopic CaCl₂ causes low workability of lime scrubber-treated MSWI-FA [18].

Presently, in many countries MSWI-FA is landfilled [19,20], but efforts are being steered towards its recovery and reuse in the production of building materials [14,21,22]. The re-valorization of MSWI-FA, or at least its safe disposal, is primarily related to being able to enhance its stability in water and curb as much as possible its heavy metal leaching,

using treatments of low environmental impact that are economically sustainable. Among the most common treatments to remove/curb chloride and heavy metals (primarily Zn, Pb, Cu, and Cd) are: washing with water, deionized, or added with basic leaching solvents [23–25]; thermal treatments in rotary kilns [26]; bioleaching (or microbial leaching, a biohydrometallurgical technology that can be applied for metal recovery) [27]; electrolytic treatments [28,29]; carbonation, reacting with CO₂ to produce stable carbonate [30]; and geo-polymerization, a geosynthetic reaction of aluminosilicate minerals in the presence of an alkali solution at low temperatures, to stabilize and immobilize fly ash [31,32].

Washing treatments, especially with acid additives, have been shown to provide the highest efficacy in terms of heavy metal removal, but they usually require a long time and a considerable amount of water (liquid/solid, L/S, ratio of 25–10 and duration of 1 h, [33]), often in combination with additives that improve the solving capacity of the solution but at the cost of managing further potential pollutants [34].

In the present work, *washing water cycles* were performed to help answer the following general question: “To which extent can the original fly ash be transformed into a product that is a non-hazardous waste, and possibly reusable, exploiting a treatment that relies upon iterative water washings only and uses comparatively small liquid/solid ratios?” In particular, the focus is on how such a treatment changes the mineralogical phase composition and heavy metal speciation distribution, to shed light on its efficacy to reduce chloride, sulfate, and heavy metal leaching from MSWI-FA.

2. Materials and Methods

2.1. Sampling and Subsampling Preparation

Fly ash was sampled at the MSW-incineration plant of Turin (Northern Italy) over a time interval of twenty weeks in 2021. A total of about 50 kg MSW-FA was quartered on site and stored at room temperature in polyethylene bottles for further analyses. Each sample used for our investigations amounted to about 1 kg; it was obtained by mixing and homogenizing fly ash by means of a laboratory riffle splitter. Eventually, sample preparation is completed by a drying cycle at 105 °C for 24 h. The particle size distribution ranges from 25 to 500 µm with a D50 ≈ 80 µm, but over 90 wt% MSW-FA lies between 250 and 53 µm (Figure S1 of Supplementary Material).

The bulk chemical composition of MSWI FA of the Turin plant was characterized by Na (27.6 wt%), Ca (12.9 wt%), Cl (10.1 wt%), S (10.3 wt%), K (4.65 wt%), and Fe (0.75 wt%) as major elements. Among heavy metals, Zn, Ti, and Pb exhibit the largest concentrations with 1.38 wt%, 0.48 wt%, and 0.311 wt%, respectively [12].

2.2. Falling Head Water Washing Implementation

Each water washing cycle is constituted by a water flow traversing MSWI-FA, implemented according to the water washing “falling head” (FH-WW) geometry (Figure 1) MSWI-FA particles are loosely packed by mechanical compacting, to have an average dry density in the range of 0.6–0.7 g/cm³. Deionized water is used to fill the free head (Chamber 1, Figure 1).

Washing water flows downwards through MSWI-FA inducing mineral dissolution reactions [35], which are affected by (i) mineral solubility and related kinetics, (ii) degree of packing, and (iii) total time of water percolation; the latter is proportional to the amount of water used. MSWI-FA is laid on a paper filter (with a thickness of 0.21 mm and a particle retention of 10–15 µm) that retains the solid fraction, letting the resulting solution pass through and be collected in the second chamber of Figure 1. Such a process is formalized by Darcy’s law [36], i.e.,

$$\frac{\Delta V}{A \times \Delta t} = \frac{\Delta h}{\Delta t} = -K \frac{h}{H} \quad (1)$$

where A = head’s section; ΔV = head’s change in Δt ; h = head’s height; Δh = height’s change in Δt ; H = thickness of the sample; K = hydraulic permeability. K has long been known to primarily depend on particle size and bulk density, both varying as a function

of time because of the changes induced by the dissolution of the mineral particles [37]. If Equation (1) is recast into its differential form and then integrated, one obtains:

$$H \times \ln\left(\frac{h(t)}{h(t_i)}\right) = - \int_{t_i}^t K(t)dt = \phi(t) \quad (2)$$

where t_i is the time at which the experiment starts and $h(t_i)$ is the height of the head at the start. A preliminary exploration of the experimental parameters (H , A and L/S = ratio between solvent mass and solid mass, at the start of the experiment) that are related to one another via

$$L/S = \frac{h(t_i) \times \rho_{liquid} \times A}{H \times \rho_{bulk} \times A} = \left(\frac{h(t_i)}{H}\right) \times \left(\frac{\rho_{liquid}}{\rho_{bulk}}\right) \quad (3)$$

where ρ_{liquid} and ρ_{bulk} are washing liquid density and MSWI-FA bulk density, respectively, has been carried out. In particular, A and H are set equal to 20 mm² and 30 mm, respectively, so that once L/S is chosen, Equation (3) allows univocal determination of $h(t_i)$, and the experimental parameter space to be explored reduces to 1D, via Equation (2). Then, the smallest L/S value that makes it possible to observe a linear dependence of $\phi(t)$ at a confidence level of at least 10σ is sought. In fact, a dependence of K on t is associated with changes of MSWI-FA's packing, induced by particle readjustment and mineral dissolution. In this case, an L/S ratio of 5 fulfills the mentioned requirements.

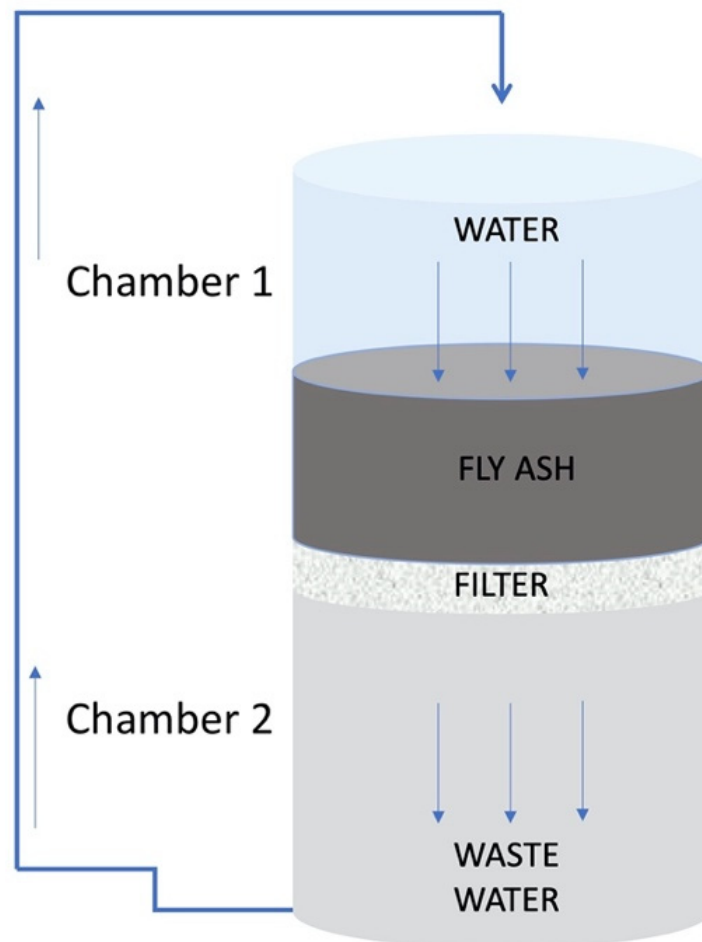


Figure 1. Scheme of the multi-step water washing.

The wastewater that is collected from percolation undergoes filtration for depuration of the contaminant species leached out from MSWI-FA, and it is then used as a regenerated solvent for a new washing step (the depuration process is outside of the present paper's

purpose). Here the focus is on the assessment of the methodology using a low electrolytic conductivity water. Specifically, attention is concentrated on (i) the role of the washing water's initial temperature (T) in relation to the kinetics of the dissolution reactions, and (ii) effects induced by washing cycles.

2.3. X-ray Powder Diffraction (XRPD)

The MSWI-FA phase composition was determined by X-ray Powder Diffraction measurements using a para-focusing geometry Rigaku Miniflex 600, with Cu-K α incident radiation, operating at 40 kV–15 mA. The diffractometer is equipped with a DTex 250 detector and optic configuration consisting of a fixed divergence slit ($1/2^\circ$) and anti-scatter slit ($1/2^\circ$). XRPD patterns were collected on pre-dried powdered samples between 2θ in the range of $3\text{--}70^\circ$, with a 2θ -step size of 0.02 and scan speed of $0.5^\circ/\text{min}$. The amorphous phase content was determined by Rietveld analysis, using high-purity calcined $\alpha\text{-Al}_2\text{O}_3$ as an internal standard (15 wt%). Data refinements were carried out by the software GSASII [38]. The Rietveld strategy involved the refinement of 15 Chebyshev polynomial background coefficients, zero parameter, cell parameters, phase fractions, isotropic crystal size, and isotropic microstrain of each phase. For some phases (i.e., gypsum), the preferential orientation effect was considered by employing the March–Dollase model implemented in GSASII. Preliminary phase identification was performed using the PDF-4 2020 database.

2.4. Washing and Leaching Tests

Water washing treatments (24 h shaking; L/S between 2 and 50) were performed in triplicate to determine the concentrations of chloride, sulfate, and heavy metals that are leached out as a function of L/S. Standard leaching tests (EN 12457-2, 2002) coincide with washing tests at L/S = 10 (i.e., 10 mL/g) and were performed on both classically water-washed samples and FH-WW samples.

Ion Chromatography (IC) measurements were carried out to measure the major anions and cations in leachates, using a Metrohm 883 Basic IC plus instrument, with a loop of 20 mL, and calibration relying upon 8 analysis spots on a reference sample (detection limit: 10 $\mu\text{g}/\text{L}$).

Inductively coupled plasma mass spectrometry (ICPMS) was performed using an Agilent 7500 ICP-MS to measure minor/trace elements with a detection limit ≤ 1 ppt for the list of analyzed elements.

2.5. Sequential Extraction Method

A modified five-step sequential extraction method [39] was employed to gain insight into heavy metal speciation distribution. Details about the procedure are provided in the Supplementary Material.

3. Results

3.1. Washing Tests

Room-temperature washing tests provide a reference for MSWI-FA dissolution as a function of L/S, assuming a constant treatment duration of 24 h; data are set out in the Supplementary Material (Table S2) and summarized in Figure 2a,b. For convenience, the leached ions are divided into two main categories: $\Sigma_{\text{major ions}}$, i.e., the sum of Na, K, Ca, Mg, bromide, fluoride, chloride, sulfate, and nitrate; and $\Sigma_{\text{heavy metals}}$, i.e., the sum of Cr, Ni, Cu, Zn, Cd, Fe, Ba, and Pb.

The $\Sigma_{\text{heavy metals}}$ exhibits high sensitivity to the L/S ratio, as suggested by a change of 75–80% on the L/S-range 5–50. This hints at an expected relevant role of L/S in promoting removal of heavy metals. As for $\Sigma_{\text{major ions}}$, a change of 25–30% occurs in the L/S-range 5–50; such a figure is comparable to the one observable in the case of weight loss.

At L/S ≥ 10 , the concentrations of chloride and sulfate become weakly dependent on time for a treatment duration over 10 min, approaching the almost invariant values of 8698 ± 100 and 3085 ± 91 mg/L, respectively, and reaching the highest EC values

(Figures S3 and S4). Conversely, heavy metals do not show definite trends as a function of washing time, as proven by the comparatively small oscillations in concentration observable in the range of 10–1440 min (average \pm e.s.d.: Cr = 6.08 ± 0.02 mg/L, Ni = 0.32 ± 0.06 mg/L, Zn = 3.99 ± 0.07 mg/L, Cd = 4.65 ± 0.05 mg/L, Fe = 22.4 ± 1.22 mg/L, Pb = 1.29 ± 0.55 mg/L).

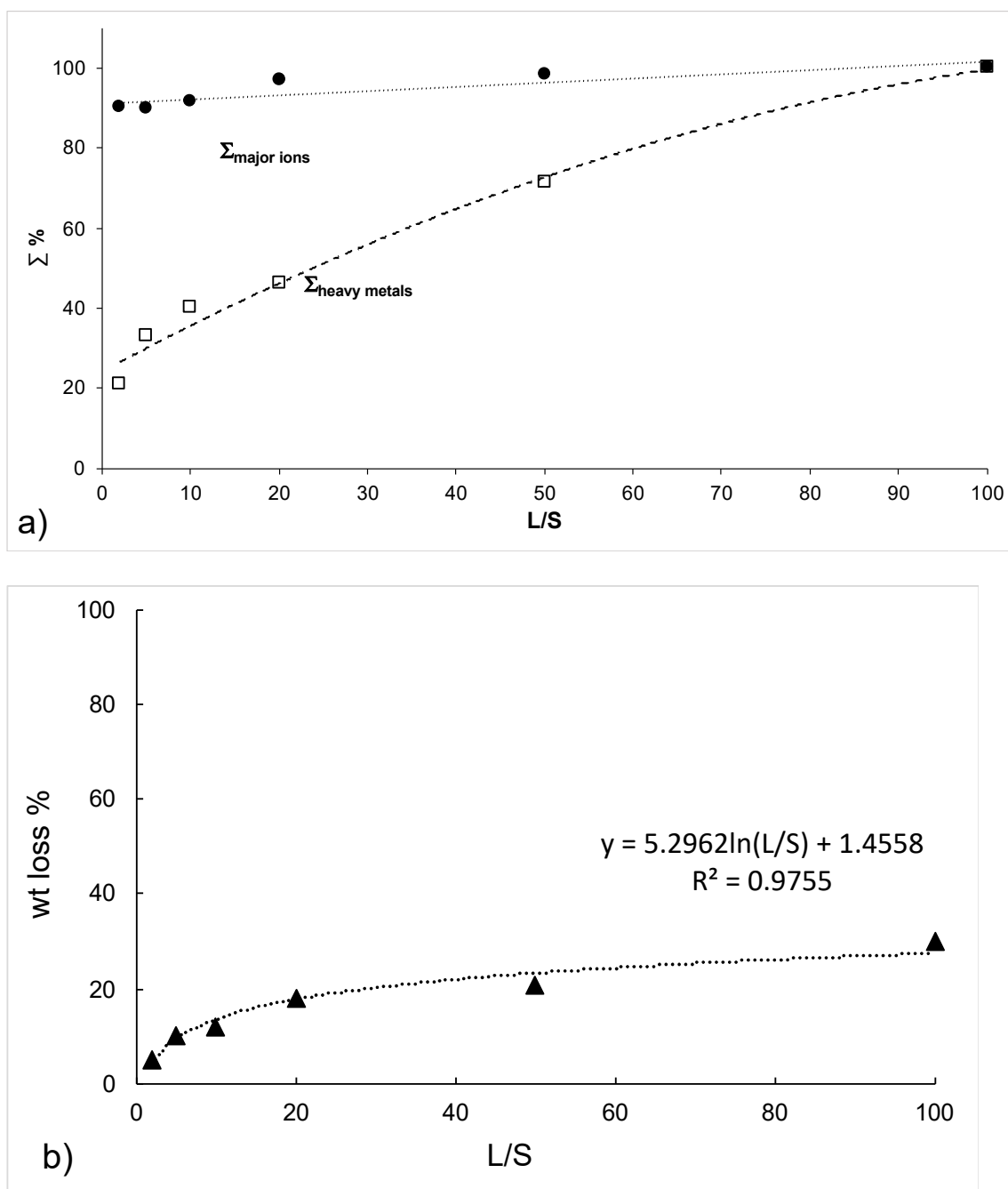


Figure 2. Washing treatments: 24 h duration. (a) $\Sigma_{\text{major ions}}$ = Na, K, Ca, Mg, bromide, fluoride, chloride, sulfate, and nitrate (filled circles), and $\Sigma_{\text{heavy metals}}$ = Cr + Ni + Cu + Zn + Cd + Fe + Ba + Pb (empty squares), versus L/S. Figures are normalized to their maximum values in terms of $\Sigma_{\text{major ions}}$ and $\Sigma_{\text{heavy metals}}$. (b) Weight loss (triangles) of MSWI-FA versus L/S because of mineral dissolution due to washing.

XRD measurements on original MSWI-FA reveal (Table 1) the occurrence of minerals such as halite (NaCl; 12 wt%), sylvite (KCl; 8 wt%), syngenite ($K_2Ca(SO_4)_2 \cdot H_2O$; 7 wt%),

anhydrite (CaSO_4 ; 10 wt%), calcite (CaCO_3 ; 6 wt%), quartz (SiO_2 ; 2 wt%), and gehlenite ($\text{Ca}_2\text{Al}_2\text{SiO}_7$; 4 wt%), along with over 50 wt% of amorphous fraction. The washing treatment induces partial hydration of anhydrite into either bassanite ($\text{CaSO}_4 \cdot 0.5\text{H}_2\text{O}$), for $L/S = 2$, or gypsum ($\text{CaSO}_4 \cdot 2\text{H}_2\text{O}$), for $L/S > 2$, while highly soluble salt (halite, sylvite, and syngenite) are almost completely dissolved for $L/S > 5$, thus resulting in a relative increase of the less soluble phases, such as quartz (5 wt%) and anhydrite (17 wt%). The fly ash particle size distribution becomes coarser after washing, since the finer fraction, represented mainly by salts, has dissolved.

Table 1. Mineralogical composition (wt%) of fly ash: fly ash before washing test and fly ash residual solid (Res) after washing test at different L/S . Crystalline phase content is estimated with an error of 1% wt, while amorphous fraction content is estimated with an error of 5% wt.

wt%	Bulk Fly Ash	Res.L/S 2	Res.L/S 5	Res.L/S 10	Res.L/S 20	Res.L/S 50
Halite	12	6	4			
Sylvite	8	2				
Calcite	6	6	6	7	8	7
Syngenite	7	5	2			
Anhydrite	10	12	13	14	15	14
Quartz	2	2	4	6	5	6
Bassanite		8				
Gypsum			11	12	10	12
Gehlenite	4	5	6	6	6	6
Amorphous	51	54	54	55	56	55

3.2. Falling Head Water Washing (FH-WW)

The change in composition of the solution from the water suspension with MSWI-FA is shown as a function of the washing steps (N_{ws}), setting $L/S = 5$, $T = 25$ or 80 °C. In particular, three classes of observables are considered, namely, pH, $C_t(\Sigma_{\text{major ions}})$, and $C_t(\Sigma_{\text{heavy metals}})$, to help point out the changes induced in MSWI-FA because of a flow of washing water. $C_t(\Sigma_{\text{major ions}})$ and $C_t(\Sigma_{\text{heavy metals}})$ define the cumulative leaching concentration as a function of the washing steps and provide a measure of the capacity of FH-WW to extract and bring into solution contaminants, thus removing them from the dry residue (Figure 3). First, it is possible to notice that water takes ~ 2 min to pass through a MSWI-FA sample at $T = 80$ °C, and ~ 4 min in the case of $T = 25$ °C, because of an increase of the dissolution kinetics with temperature, thus accelerating percolation. All this is in keeping with the fact that, at 80 °C, the weight loss after 5 and 12 washing steps is 18 and 21 wt%, respectively; such figures change into 17 and 19% at room temperature. In all cases (Figure 3, top and bottom) the cumulative leaching concentration increases very rapidly and then shows steady trends: quasi-flat for $\Sigma_{\text{major ions}}$ versus relatively steep for $\Sigma_{\text{heavy metals}}$, the latter exhibiting a T-dependent slope ($dC_t(\Sigma_{\text{heavy metals}})/dN_{ws} = 0.612$ and $2.603 \text{ mgL}^{-1}/\text{cycle}$, for $T = 25$ and 80 °C, respectively; N_{ws} -range = 5–12).

The concentration trends qualitatively suggest that: (i) the effect of temperature is modest on chloride and sulfate removal, while becoming more relevant for heavy metals; (ii) the achievement of a quasi-steady state for most of the ions is observable after 6–7 washing cycles, though Ca^{2+} , Pb , Zn , and SO_4^{2-} continue slightly increasing their concentrations from the ninth washing treatment onwards. Conversely, the pH trend, expressed as the average between the values measured at $T = 25$ °C and 80 °C, oscillates around a basic value of the averaged value of 11.2 ± 0.4 (Figure 4) and stabilizes around 10.9 (Figure 4).

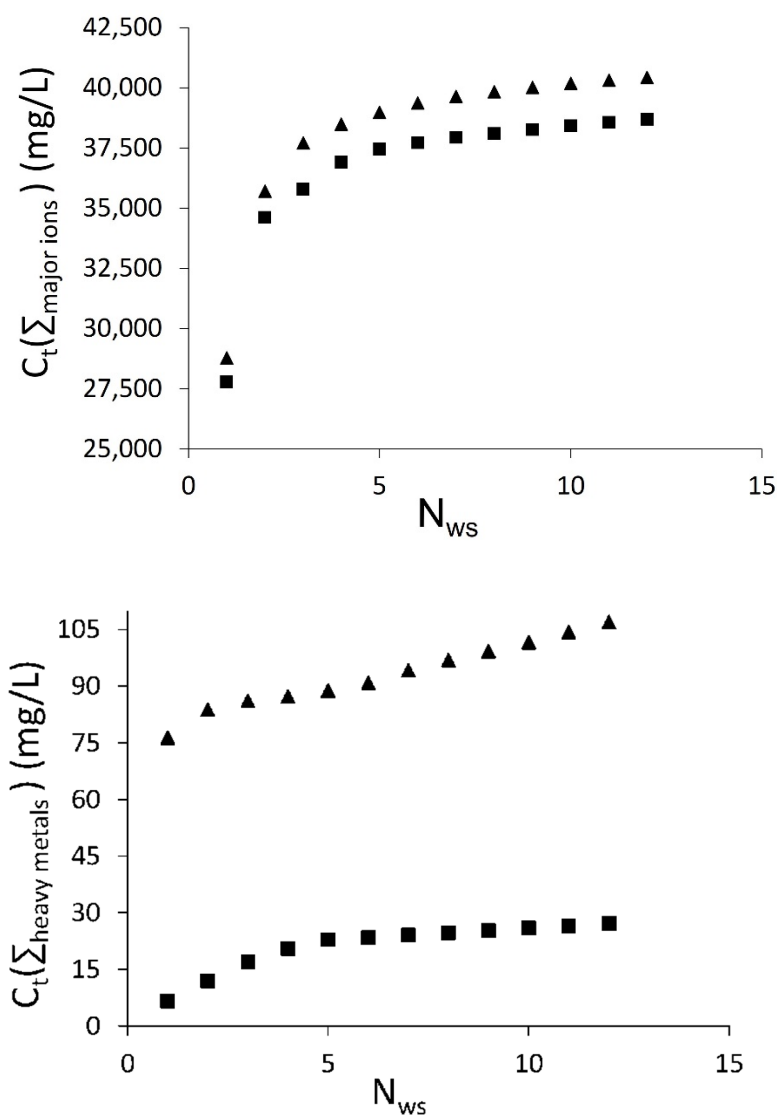


Figure 3. Cumulative leaching concentration (C_t) $\Sigma_{\text{major ions}}$, top, and $\Sigma_{\text{heavy metals}}$, bottom, versus number of washing steps (N_{ws}) at 25 (squares) and 80 °C (triangles).

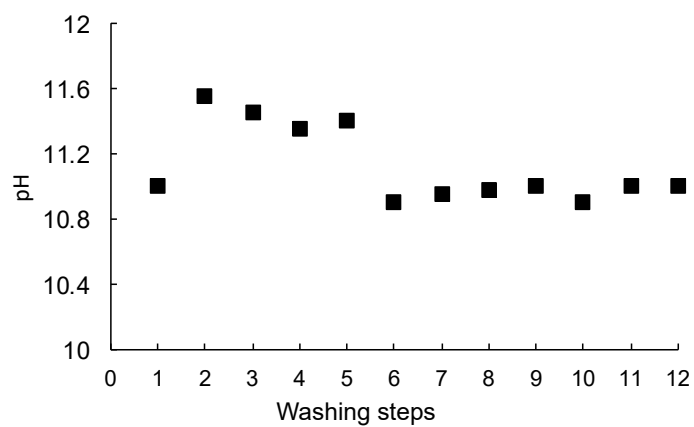


Figure 4. Average pH values as a function of N_{ws} (number of washing steps).

3.3. Leaching Tests

Leaching tests (Table 2), applied to the dry solid residue after FH-WW (N_{ws} up to 30), show that Cr, Ni, Cd, sulfate, and fluoride are still over the Italian legal limits for reuse [38].

Comparing $N_{ws} = 5$ with $N_{ws} = 12$, a significant difference is apparent in the case of Na, K, Ca, chloride, sulfate, and Cr, which exhibit high sensitivity to dilution.

Table 2. Leaching test (L/S = 10) of the solid residue of FA after five- and twelve-step FH-WW at 80 °C and five-, twelve-, and thirty-step FH-WW at 25 °C. Explanation 1: $N_{ws} = 5$, L/S = 5, T = 80 °C; 2: $N_{ws} = 12$, L/S = 5, T = 80 °C; 3: $N_{ws} = 5$, L/S = 5, T = 25 °C; 4: $N_{ws} = 12$, L/S = 5, T = 25 °C; 5: $N_{ws} = 30$, L/S = 5, T = 25 °C; 6: 24 h washing L/S = 50, T = 25 °C; 24 h washing, L/S = 5, T = 25 °C. Legal limits according to: [40,41].

	1	2	3	4	5	6	7	Not Reactive [40]	Non Hazardous [40]	Hazardous	Reuse [41]
E.Cond. ($\mu\text{s}/\text{cm}$)	1650	1037	1858	1500	1340	1400	3160				
pH	9.6	9.6	9.7	9.2	9.2	9.1	9.4				5.5–12
Na (mg/L)	36	15	45	25	20	41	167				
K(mg/L)	37	31	58	15	9	31	159				
Ca (mg/L)	440	240	409	329	311	273	365				
Mg (mg/L)	0.3	0.2	0.3	0.3	0.2	0.6	7				
Chloride (mg/L)	51	43	100	83	73	125	500	80	2500	2500	100
Bromides (mg/L)	0.5	n.d.	3.4	2.8	n.d.	1.1	n.d.				
Fluorides (mg/L)	n.d.	1.1	1.7	2	1.2	0.5	n.d.	1	15	50	1.5
Sulfate (mg/L)	574	431	860	662	578	475	920	100	5000	5000	250
NO_3^- (mg/L)	0.4	n.d.	n.d.	0.8	n.d.	1.3	n.d.				50
Cr (mg/L)	0.18	0.10	0.08	0.03	0.06	0.13	0.25	0.05	1	7	0.05
Ni (mg/L)	0.09	0.08	0.02	n.d.	0.05	0.06	0.11	0.04	1	4	0.01
Cu (mg/L)	0.04	0.05	n.d.	n.d.	n.d.	n.d.	n.d.	0.2	5	10	0.05
Zn (mg/L)	0.1	0.2	n.d.	n.d.	0.005	0.05	0.04	4	5	20	3
Cd (mg/L)	0.02	0.02	n.d.	n.d.	n.d.	n.d.	n.d.	0.004	0.1	0.5	0.005
Ba (mg/L)	0.12	0.12	0.04	0.08	0.06	0.11	0.1	2	10	30	1
Pb (mg/L)	0.04	0.05	n.d.	n.d.	n.d.	0.005	n.d.	0.05	1	5	0.05

At T = 25 °C, leaching tests indicate that a five-step treatment is not sufficient to reduce Cr, Ni, Cd, fluoride, and sulfate below the legislation limits for reuse (Table 2). Conversely, a twelve-step treatment gives leachates in which all the analyzed heavy metals lie under the legal limits, along with chloride, whereas only sulfate still lies above the limit (Table 2).

For comparison, the leachates of a conventional water washing treatment of fly ash at L/S 50 and 24 h versus a thirty-step washing test at T = 25 °C are reported in Table 2 and Figure 5; a modest decrease both of chloride and sulfate is observable, with respect to $N_{ws} = 12$. Note that the case of $N_{ws} = 80$ (not reported here) still shows a sulfate concentration over the legal limit for reuse. The extrapolation of the sulphate concentration versus N_{ws} proves that a number of washing steps as large as 370 is required to have a leachate within the legal limits for reuse. As to the heavy metals, no significant decrease is observable when comparing $N_{ws} = 12$ with $N_{ws} = 30$.

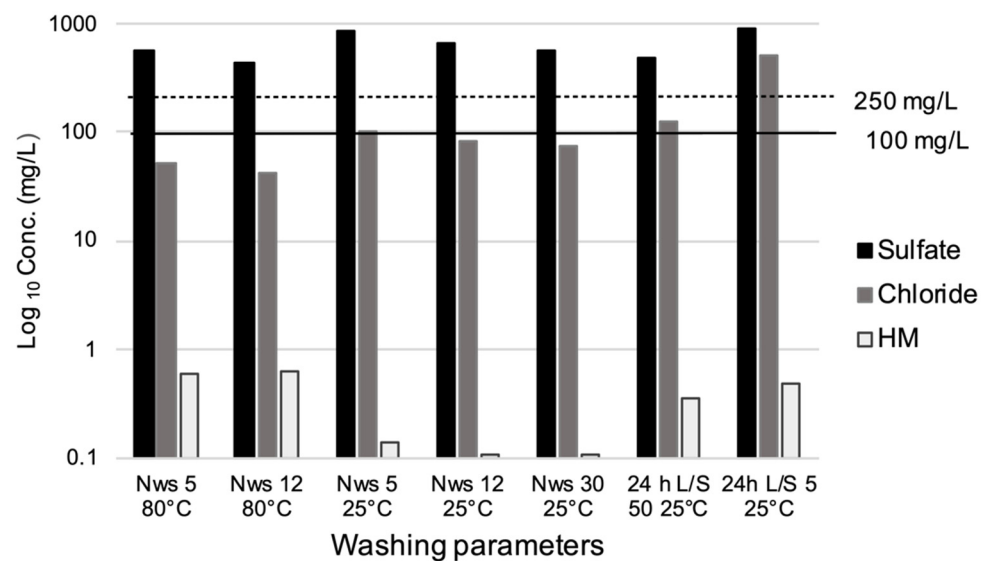


Figure 5. Leaching tests on FA treated by FH-WW, as a function of temperature (25–80 °C) and N_{ws} (5–30); for comparison, the cases of 24 h washing with L/S = 50 and 5 are reported. Attention is focused on chloride, sulfate, and heavy metal (HM) concentrations. Dotted line and solid line: legal limits for reuse in the case of sulfate (250 mg/L) and chloride (100 mg/L), respectively.

4. Discussion

The FH-WW related phenomenology can be better analyzed by employing the kinetics reaction formalism and using the cumulative leaching concentrations as experimental variables (Figure 3).

In a liquid/solid reaction system, the kinetics rate is generally influenced by chemical species diffusion through the solvent, diffusion through the solid layer, and/or possible chemical reactions at the solid particles' surface [42]. This is described by the shrinking core model (SCM), which assumes homogeneous spherical particles and derives two formulations to take chemical reactions or diffusion through the outer layer into account [43,44]:

$$1 - (1 - \alpha)^{\frac{1}{3}} = k_R t \quad (4)$$

$$1 - 3(1 - \alpha)^{\frac{2}{3}} + 2(1 - \alpha) = k_D t \quad (5)$$

where α represents the relative cumulative leaching with respect to the maximum after 12 steps; k_D (diffusion) and k_R (reactions) are the reaction rate constants; t is the time calculated by multiplying the number of steps by the mean water contact time (i.e., 4 and 2 min for 25 and 80 °C, respectively). Table 3 and Figure S5 show how the second SCM formulation better fits both heavy metals and major ions data, though all the correlation coefficients are not ideal ($R^2 < 0.95$).

Table 3. Linear correlation coefficient of SCM plots.

	Temperature (°C)	R^2 (R)	R^2 (D)
$\Sigma_{\text{heavy metals}}$	25	0.93	0.93
	80	0.91	0.93
$\Sigma_{\text{major ions}}$	25	0.91	0.93
	80	0.92	0.94

Considering the cumulative leaching concentration trends, it is possible to parametrize the process by a second-order rate law. This empirical approach has been successfully

employed in similar fields, involving heavy metals extraction from sludge [45,46]. After [47] the formulation can be written as:

$$\frac{dC_t}{dt} = k(C_s - C_t)^2 \quad (6)$$

$$\frac{t}{C_t} = \frac{1}{kC_s^2} + \frac{t}{C_s} \quad (7)$$

where C_t represents the cumulative leaching concentration at time t , k is the leaching rate constant, and C_s the cumulative leaching concentration at saturation conditions (i.e., $t \rightarrow \infty$, which implies $N_{ws} \rightarrow \infty$). The resulting plots are displayed in Figure 6, where good agreement between model and experiments is proven by the high correlation coefficient in all cases ($R^2 > 0.98$).

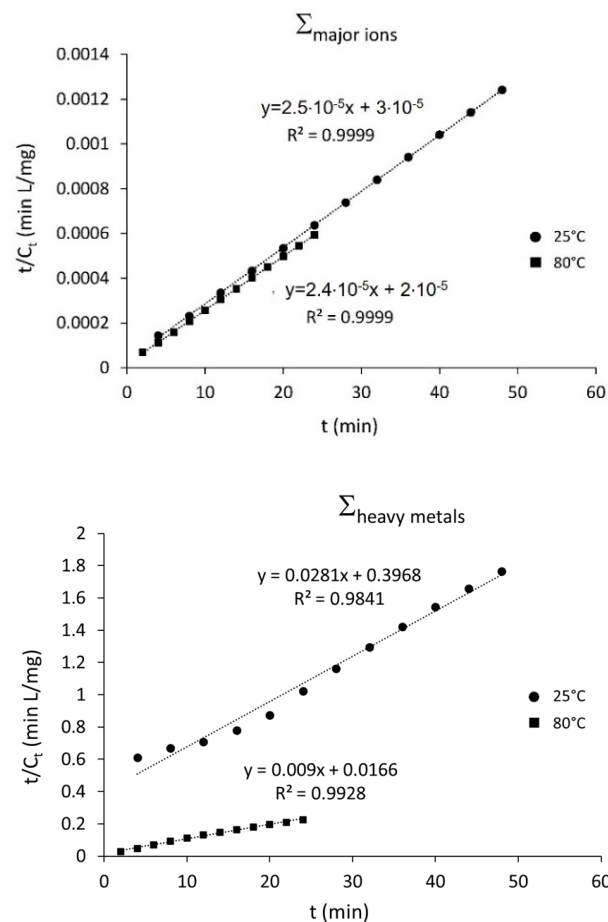


Figure 6. Empirical second-order reaction model plots for $\Sigma_{\text{heavy metals}}$ (bottom) and $\Sigma_{\text{major ions}}$ (top).

The leaching rate constants (Table 4) were calculated by slope and intercept of the lines of Figure 6, to extract the apparent E_a of the process by the Arrhenius linearized equation:

$$k = Ae^{\frac{E_a}{RT}} \quad (8)$$

$$\ln(k) = \ln(A) + \frac{E_a}{RT} \quad (9)$$

where A = pre-exponential factor, E_a = apparent activation energy, R = gas constant and T = absolute temperature. Although two temperatures suffice to extract E_a , they do not provide a robust statistical assessment. Nonetheless, E_a was tentatively calculated for both major ions and heavy metals to roughly evaluate its order of magnitude, but leaving any claim of precision aside. The results are set out in Table 5 and Figure S6. A diffusion-like

process usually exhibits an $E_a < 20$ kJ/mol, while a chemical reaction commonly yields $E_a > 40$ kJ/mol [43,44]. In both cases, the relatively low activation energies obtained here seem to suggest that the leaching rates of both heavy metals and major ions are mainly controlled by physical/diffusion processes.

Table 4. Kinetical parameters derived from the empirical second-order reaction model.

	Cs (mg/L)	k (L mg ⁻¹ min ⁻¹)	R^2
$\Sigma_{\text{heavy metals}}$	35.71	3.2×10^3	0.9841
	111.11	7.4×10^5	0.9982
$\Sigma_{\text{major ions}}$	40,000	5.3×10^{13}	0.9999
	42,478	7.2×10^{13}	0.9999

Table 5. Activation energy derived by Arrhenius Equation (9).

	$\ln k$	$1/T$ (K ⁻¹)	E_a (KJ/mol)
$\Sigma_{\text{heavy metals}}$	8.075	3.2×10^{-3}	1.25
	13.52	2.8×10^{-3}	
$\Sigma_{\text{major ions}}$	31.6	3.2×10^{-3}	0.104
	31.9	2.8×10^{-3}	

The relevant difference between the curves' slopes at the beginning ($N_{ws} < 5$) and at the end ($N_{ws} > 5$) of the washing process in Figure 3 suggests that the reaction is divided into two stages: (i) an intense and fast dissolution occurs at the start, due to the scrubbing action of the water flow and the soluble salt clustering on particle surface, as shown [12]; (ii) a slower chemical species diffusion develops from solid into solution, successively.

Leaching tests on FH-WW treated samples (Table 2 and Figure 5) indicate that FH-WW at 25 °C gives a dry product that is less prone to heavy metal leaching than its counterpart at 80 °C. Although such an issue is unexpected, it is confirmed by full reproducibility of the observations. This effect is, in our opinion, engendered by the residue of incomplete dissolution reactions boosted by high temperature and interrupted before completion because of kinetic reasons, thus leaving the solid portion still reactive to water (Figure 3 bottom).

A comparison with conventional single-step washing treatments at $L/S = 50$ and $L/S = 5$ (duration: 24 h) shows the higher efficiency of FH-WW on chloride and heavy metal removal. In particular, by comparing the washing treatment relying on $L/S = 50$ and $t = 24$ h against FH-WW with $N_{ws} = 30$, it is evident that FH-WW not only provides an improvement in terms of dry product leaching (chloride and heavy metals), but also allows saving both water ($L/S = 50$ versus 5) and time (24 versus 2.5 h).

MSWI-FA is easily converted into non-hazardous waste, whereas it is more complex to achieve the conditions required for non-reactive waste. In particular, sulfate is the contaminant that shows the lowest sensitivity to those of FH-WW's parameters (temperature and N_{ws}) that are technologically manageable. An increase in the L/S ratio, i.e., a dilution of the solution, leads to a decrease in leachate's sulfate concentration, as proven by the leaching tests on fly ash treated with $L/S = 5$ and 50; yet, this is a strategy difficult to be developed on a large scale.

The phase compositions of the FA after FH-WW (Table 6) do not show significant differences between samples washed with five- or twelve-step treatments, at 25 and 80 °C, in terms of occurring minerals and their relative amounts. In all cases, the soluble chloride is not detectable anymore, while the most abundant crystalline phase is represented by anhydrite that is not associated with any of its hydration products, such as bassanite and gypsum. This is likely related to the off-equilibrium conditions due to the kinetics driving the process. Conversely, the standard washing treatment (static batch and 24 h duration) provides better approximate equilibrium conditions. Nonetheless, the relatively large amount of anhydrite and its slow kinetics of dissolution [48] are probably the reason why there is still relevant sulfate concentration in leachates even after 30 steps.

Table 6. Mineralogical composition (wt%) of fly ash after FH-WW. Crystalline phase content is estimated with an error of 1% wt, while amorphous fraction content is estimated with an error of 5% wt.

wt%	5-Step at 25 °C	12-Step at 25 °C	5-Step at 80 °C	12-Step at 80 °C	30-Step
Calcite	8	7	9	8	6
Anhydrite	15	14	17	16	13
Quartz	8	10	7	10	10
Gehlenite	7	8	8	7	9
Amorphous	62	61	60	59	62

The MSWI-FA leaching of heavy metals is rationalized through their speciation distribution, which was obtained by the five-class sequential extraction method. The five classes are defined as follows: easily exchangeable (F0), carbonates (F1), reducible (F2), oxidizable (F3), and residual (F4). F0 and F1 point to speciation types that are prone to a comparatively low acidic dissolution and, hence, are potentially responsible for most of the heavy metal leaching. F4 speciation is associated with virtually insoluble phases, unless a very strong acid attack is used [39]. F2 and F3 speciation types are intermediate between F1 and F4. In so doing, the speciation distribution of pristine MSWI-FA, five- and twelve-step washing treatments at 80 °C, was determined. All the results from sequential extraction experiments are shown in Figure 7.

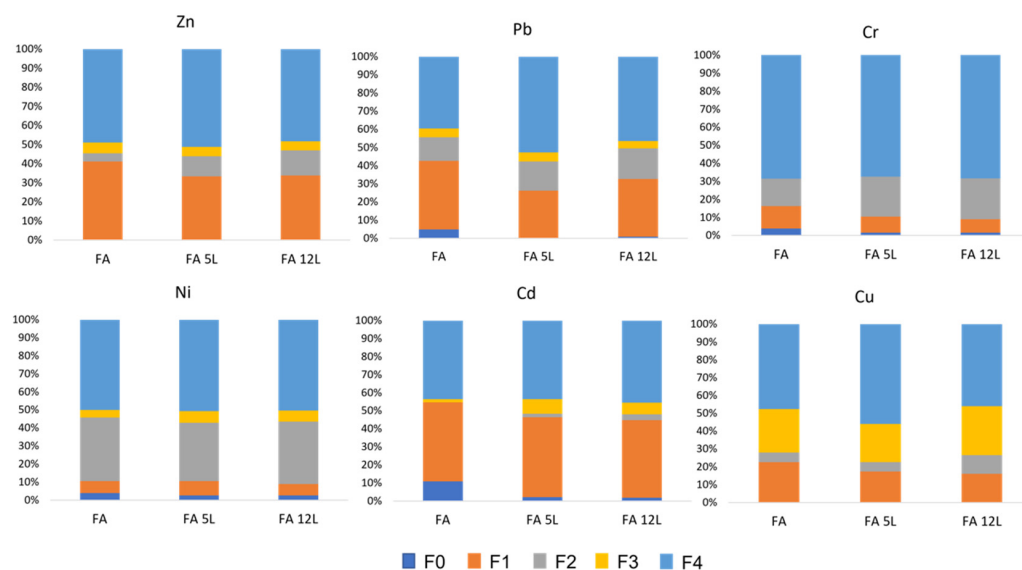


Figure 7. Speciation distribution of the main heavy metals for pristine FA and FA that underwent five- and twelve-step washing treatments at 80 °C. 5 L: $N_{ws} = 5$; 12 L: $N_{ws} = 12$.

Leaching tendency is mainly correlated with F0 and F1, which represent the fractions associated with crystal/glass particles prone to species exchange and carbonate, respectively [49]. Although F4 provides the highest fraction percentage for all heavy metals (between 40–65%), it is constituted of very low soluble phases, and therefore gives a relatively modest contribution to leaching. Conversely, the average large values of F0 + F1, which lie over 20% for most species, can explain the observed relevant heavy metal leaching. The FH-WW treatment markedly reduces the contribution of F0 and, to a lesser extent, F1's. The largest reduction involves Pb (16%) and is associated with chloride and carbonate [50,51]. For $N_{ws} > 5$, a steady improvement is not observed in terms of leaching reduction, save at the cost of a significant increase in the washing cycles (see Figure 3). Eventually, in the case of Ni, Cr, and Cd, the residual F0 + F1 cumulative fraction (15–50%) is sufficient to leach out heavy metals whose concentrations lie above the legislated limits for FA reuse.

5. Conclusions

Falling head water washing (FH-WW) treatment was investigated to reduce chloride, sulfate, and heavy metal leaching from municipal solid waste incineration fly ash, which has a phase composition provided by amorphous (50 wt%), halite (12 wt%), sylvite (8 wt%), anhydrite (10 wt%), and, to a lesser extent, by quartz, calcite, and gehlenite (12 wt%).

FH-WW relies upon soluble phase dissolution and removal of the related species that are dragged away by the gravity-driven flow of solvent traversing a FA sample. This is shown by the speciation distribution analysis, which proves the changes in terms of chloride/sulfate/heavy metals leaching from FA to be related to a reduction of the F0 + F1 solid fraction, i.e., ion exchangeable and carbonate phases. Dissolution kinetics is the key reaction governing the cleaning process of FH-WW, which, in this respect, differs much from conventional washing that takes place at quasi-equilibrium conditions. A more detailed analysis by employing an empirical second-order kinetics model suggests that a two-step mechanism is involved. At first, a very fast dissolution occurs, related to the readily soluble fraction present on the FA particle surface, followed by a much slower diffusion step. FH-WW yields a dry product with reduced contaminant leaching with respect to that from FA treated using conventional washing at L/S = 50 for 24 h, thus providing comparatively relevant water (L/S = 5 versus 50) and time (2.5 versus 24 h) savings. The use of high-temperature water in FH-WW, i.e., 80 °C, does not provide significant enhancement in terms of leaching behaviour of the treated FA. Altogether, room temperature FH-WW is a successful strategy to take chloride and many heavy metals below the legal limits for reuse, whereas it fails for sulfate, Cr, and Ni. However, not all contaminants are reduced below the legal limits required for a non-hazardous waste classification. Improvements are expected if washing is carried out by shifting washing water to a more acidic regime.

Supplementary Materials: The following supporting information can be downloaded at: <https://www.mdpi.com/article/10.3390/min12060742/s1>, Figure S1: Particle size distribution of fly ash; Table S1: Sequential extraction method parameters; Table S2: Concentration of fly ash washing solutions; Figure S3: Time (min) *versus* EC ($\mu\text{S}/\text{cm}$) of fly ash washing test; Figure S4: Detail of figure S3 at time 0–30 min; Table S5: Mineralogical composition (wt%) of fly ash; Table S6: Mineralogical composition (wt%) of fly ash after FH-WW; Figure S5: SCM plots when chemical reactions (left) or diffusion (right) are considered the rate-determining step; Figure S6: Arrhenius plot.

Author Contributions: Conceptualization, C.C., D.B., E.D., A.P., C.B. and L.P.; methodology, C.C., D.B., E.D., C.B. and A.P.; software, C.C., D.B. and E.D.; validation, C.C., D.B., E.D., C.B., A.P. and L.P.; formal analysis, C.C., D.B., E.D., C.B. and A.P.; investigation, C.C., D.B., E.D., C.B. and A.P.; resources, C.C., D.B., E.D., L.P. and C.B.; data curation, C.C., D.B., E.D., C.B., A.P. and L.P.; writing—original draft preparation, C.C., D.B. and A.P.; writing—review and editing, C.C., D.B., E.D., C.B., A.P. and L.P.; visualization, C.C., D.B., E.D. and A.P.; supervision, A.P., E.D., C.B. and L.P.; project administration, A.P.; funding acquisition, A.P. All authors have read and agreed to the published version of the manuscript.

Funding: This research was funded by Università degli Studi di Torino (Italy), IREN S.p.A. (Italy), Ecospray S.p.A. (Italy) and Italian Ministry for Education, University and Research (MUR; project PRIN2017-2017L83S77), for water washing apparatus; by Ministry for Ecological Transition (MiTE; project CLEAN), for investigations on general properties of fly ash.

Institutional Review Board Statement: Not applicable.

Informed Consent Statement: Not applicable.

Data Availability Statement: Not applicable.

Acknowledgments: D.B. wishes to thank Quentin Wehrung for useful suggestions. The authors are grateful to four anonymous referees for comments and observations that significantly improved the quality of the original manuscript.

Conflicts of Interest: The authors declare no conflict of interest. The funders had no role in the design of the study; in the collection, analyses, or interpretation of data; in the writing of the manuscript, or in the decision to publish the results.

References

1. Quina, M.J.; Bontempi, E.; Bogush, A.; Schlumberger, S.; Weibel, G.; Braga RFunari, V.; Hyks, J.; Rasmussen, E.; Lederer, J. Technologies for the management of MSW incineration ashes from gas cleaning: New perspectives on recovery of secondary raw materials and circular economy. *Sci. Total Environ.* **2018**, *635*, 526–542. [[CrossRef](#)] [[PubMed](#)]
2. Parashar, C.K.; Das, P.; Samanta, S.; Ganguly, A.; Chatterjee, P.K. Municipal Solid Wastes—A Promising Sustainable Source of Energy: A Review on Different Waste-to-Energy Conversion Technologies. In *Energy Recovery Processes from Wastes*; Ghosh, S., Ed.; Springer: Singapore, 2020. [[CrossRef](#)]
3. Joseph, A.M.; Snellings, R.; Van den Heede, P.; Matthys, S.; De Belie, N. The Use of Municipal Solid Waste Incineration Ash in Various Building Materials: A Belgian Point of View. *Materials* **2018**, *11*, 141. [[CrossRef](#)] [[PubMed](#)]
4. Lam, C.H.; Ip, A.W.; Barford, J.P.; McKay, G. Use of incineration MSW ash: A review. *Sustainability* **2010**, *2*, 1943–1968. [[CrossRef](#)]
5. Directive 2008/98/EC of the European Parliament and of the Council of 19 November 2008 on Waste and Repealing Certain Directives. Available online: <https://eur-lex.europa.eu/legal-content/EN/TXT/?uri=CELEX%3A02008L0098-20180705> (accessed on 9 April 2022).
6. Dontrios, S.; Likitlersuang, S.; Janjaroen, D. Mechanisms of chloride and sulfate removal from municipal-solid-waste-incineration fly ash (MSWI FA): Effect of acid-base solutions. *Waste Manag.* **2020**, *101*, 44–53. [[CrossRef](#)]
7. Zhao, K.; Hu, Y.; Tian, Y.; Chen, D.; Feng, Y. Chlorine removal from MSWI fly ash by thermal treatment: Effects of iron/aluminum additives. *J. Environ. Sci.* **2020**, *88*, 112–121. [[CrossRef](#)]
8. Ni, P.; Xiong, Z.; Tian, C.; Li, H.; Zhao, Y.; Zhang, J.; Zheng, C. Influence of carbonation under oxy-fuel combustion flue gas on the leachability of heavy metals in MSWI fly ash. *Waste Manag.* **2017**, *67*, 171–180. [[CrossRef](#)]
9. Hu, H.Y.; Liu, H.; Shen, W.Q.; Luo, G.Q.; Li, A.J.; Lu, Z.L.; Yao, H. Comparison of CaO's effect on the fate of heavy metals during thermal treatment of two typical types of MSWI fly ashes in China. *Chemosphere* **2013**, *93*, 590–596. [[CrossRef](#)]
10. Nikravan, M.; Ramezaniapour, A.A.; Maknoon, R. Study on physicochemical properties and leaching behavior of residual ash fractions from a municipal solid waste incinerator (MSWI) plant. *J. Environ. Manag.* **2020**, *260*, 110042. [[CrossRef](#)]
11. Loginova, E.; Proskurnin, M.; Brouwers, H.J.H. Municipal solid waste incineration (MSWI) fly ash composition analysis: A case study of combined chelant-based washing treatment efficiency. *J. Environ. Manag.* **2019**, *235*, 480–488. [[CrossRef](#)]
12. Bernasconi, D.; Caviglia, C.; Destefanis, E.; Agostino, A.; Boero, R.; Marinoni, N.; Bonadiman, C.; Pavese, A. Influence of speciation distribution and particle size on heavy metal leaching from MSWI fly ash. *Waste Manag.* **2022**, *138*, 318–327. [[CrossRef](#)]
13. Ginés, O.; Chimenos, J.M.; Vizcarro, A.; Formosa, J.; Rosell, J.R. Combined use of MSWI bottom ash and fly ash as aggregate in concrete formulation: Environmental and mechanical considerations. *J. Hazard. Mater.* **2009**, *169*, 643–650. [[CrossRef](#)] [[PubMed](#)]
14. Colangelo, F.; Messina, F.; Cioffi, R. Recycling of MSWI fly ash by means of cementitious double step cold bonding pelletization: Technological assessment for the production of lightweight artificial aggregates. *J. Hazard. Mater.* **2015**, *299*, 181–191. [[CrossRef](#)] [[PubMed](#)]
15. Yakubu, Y.; Zhou, J.; Ping, D.; Shu, Z.; Chen, Y. Effects of pH dynamics on solidification/stabilization of municipal solid waste incineration fly ash. *J. Environ. Manag.* **2018**, *207*, 243–248. [[CrossRef](#)] [[PubMed](#)]
16. Ferraro, A.; Farina, I.; Race, M.; Colangelo, F.; Cioffi, R.; Fabbicino, M. Pre-treatments of MSWI fly-ashes: A comprehensive review to determine optimal conditions for their reuse and/or environmentally sustainable disposal. *Rev. Environ. Sci. Biotechnol.* **2019**, *18*, 453–471. [[CrossRef](#)]
17. Zhou, Y.; Gencturk, B.; Willam, K.; Attar, A. Carbonation-induced and chloride-induced corrosion in reinforced concrete structures. *J. Mater. Civ. Eng.* **2015**, *27*, 04014245. [[CrossRef](#)]
18. Cho, B.H.; Nam, B.H.; An, J.; Youn, H. Municipal Solid Waste Incineration (MSWI) Ashes as Construction Materials—A Review. *Materials* **2020**, *13*, 3143. [[CrossRef](#)]
19. Zhang, Y.; Ma, Z.; Fang, Z.; Qian, Y.; Zhong, P.; Yan, J. Review of harmless treatment of municipal solid waste incineration fly ash. *Waste Dispos. Sustain. Energy* **2020**, *2*, 1–25. [[CrossRef](#)]
20. Assi, A.; Bilo, F.; Zanoletti, A.; Ponti, J.; Valsesia, A.; La Spina, R.; Zacco, A.; Bontempi, E. Zero-waste approach in municipal solid waste incineration: Reuse of bottom ash to stabilize fly ash. *J. Clean. Prod.* **2020**, *245*, 118779. [[CrossRef](#)]
21. Yin, K.; Ahamed, A.; Lisak, G. Environmental perspectives of recycling various combustion ashes in cement production—A review. *Waste Manag.* **2018**, *78*, 401–416. [[CrossRef](#)]
22. Chen, W.; Klupsch, E.; Kirkelund, G.M.; Jensen, P.E.; Ottosen, L.M.; Dias-Ferreira, C. Recycling of MSWI fly ash in clay bricks-effect of washing and electro-dialytic treatment. In *WASTES—Solutions, Treatments and Opportunities II*; Taylor & Francis: Abingdon, UK, 2017; pp. 183–189.
23. Kang, D.; Son, J.; Yoo, Y.; Park, S.; Huh, I.-S.; Park, J. Heavy-metal reduction and solidification in municipal solid waste incineration (MSWI) fly ash using water, NaOH, KOH, and NH₄OH in combination with CO₂ uptake procedure. *Chem. Eng. J.* **2020**, *380*, 122534. [[CrossRef](#)]
24. Nordmark, D.; Lagerkvist, A. Controlling the mobility of chromium and molybdenum in MSWI fly ash in a washing process. *Waste Manag.* **2018**, *76*, 727–733. [[CrossRef](#)] [[PubMed](#)]

25. Chen, X.; Bi, Y.; Zhang, H.; Wang, J. Chlorides Removal and Control through Water-washing Process on MSWI Fly Ash. *Procedia Environ. Sci.* **2016**, *31*, 560–566. [[CrossRef](#)]
26. Huber, F.; Blasenbauer, D.; Mallow, O.; Lederer, J.; Winter, F.; Fellner, J. Thermal co-treatment of combustible hazardous waste and waste incineration fly ash in a rotary kiln. *Waste Manag.* **2016**, *58*, 181–190. [[CrossRef](#)] [[PubMed](#)]
27. Gomes, H.I.; Funari, V.; Ferrari, R. Bioleaching for resource recovery from low-grade wastes like fly and bottom ashes from municipal incinerators: A SWOT analysis. *Sci. Total Environ.* **2020**, *715*, 136945. [[CrossRef](#)] [[PubMed](#)]
28. Kirkelund, G.M.; Skevi, L.; Ottosen, L.M. Electrodialytically treated MSWI fly ash use in clay bricks. *Constr. Build. Mater.* **2020**, *254*, 119286. [[CrossRef](#)]
29. Huang, T.; Zhou, L.; Liu, L.; Xia, M. Ultrasound-enhanced electrokinetic remediation for removal of Zn, Pb, Cu and Cd in municipal solid waste incineration fly ashes. *Waste Manag.* **2018**, *75*, 226–235. [[CrossRef](#)]
30. De Boom, A.; Aubert, J.E.; Degrez, M. Carbonation of municipal solid waste incineration electrostatic precipitator fly ashes in solution. *Waste Manag. Res.* **2014**, *32*, 406–413. [[CrossRef](#)]
31. Zhan, X.; Wang, L.; Wang, L.; Wang, X.; Gong, J.; Yang, L.; Bai, J. Enhanced geopolymeric co-disposal efficiency of heavy metals from MSWI fly ash and electrolytic manganese residue using complex alkaline and calcining pre-treatment. *Waste Manag.* **2019**, *98*, 135–143. [[CrossRef](#)]
32. Zheng, L.; Wang, C.; Wang, W.; Shi, Y.; Gao, X. Immobilization of MSWI fly ash through geopolymerization: Effects of water-wash. *Waste Manag.* **2011**, *31*, 311–317. [[CrossRef](#)]
33. Phua, Z.; Giannis, A.; Dong, Z.L.; Lisak, G.; Ng, W.J. Characteristics of incineration ash for sustainable treatment and reutilization. *Environ. Sci. Pollut. Res.* **2019**, *26*, 16974–16997. [[CrossRef](#)]
34. Kanhar, A.H.; Chen, S.; Wang, F. Incineration Fly Ash and its treatment to possible utilization: A review. *Energies* **2020**, *13*, 6681. [[CrossRef](#)]
35. Li, L.; Steefel, C.I.; Yang, L. Scale dependence of mineral dissolution rates within single pores and fractures. *Geochim. Cosmochim. Acta* **2008**, *72*, 360–377. [[CrossRef](#)]
36. Atangana, A. Chapter 2: Principle of Groundwater Flow. In *Fractional Operators with Constant and Variable Order with Application to Geo-Hydrology*; Atangana, A., Ed.; Academic Press: Cambridge, MA, USA, 2018; pp. 15–47, ISBN 9780128096703. [[CrossRef](#)]
37. Chen, L.; Kang, Q.; Viswanathan, H.S.; Tao, W.Q. Pore-scale study of dissolution-induced changes in hydrologic properties of rocks with binary minerals. *Water Resour. Res.* **2014**, *50*, 9343–9365. [[CrossRef](#)]
38. Toby, B.H.; Van Dreele, R.B. GSAS-II: The genesis of a modern open-source all purpose crystallography software package. *J. Appl. Cryst.* **2013**, *46*, 544–549. [[CrossRef](#)]
39. Bruder-Hubscher, V.; Lagarde, F.; Leroy, M.J.F.; Coughanowr, C.; Enguehard, F. 523 Application of a sequential extraction procedure to study the release of elements from municipal solid waste incineration bottom ash. *Anal. Chim. Acta* **2002**, *451*, 285–525. [[CrossRef](#)]
40. Ministerial Decree n. 186 Dated 5 April 2006. Regulatory That Modified Ministerial Decree Dated 5 February 1998. *Official Gazette n. 115*. 19 May 2006. Available online: <http://www.gazzettaufficiale.it/eli/gu/2010/12/01/281/sg/pdf> (accessed on 9 April 2022).
41. G.U. Ministerial Decree 27/09/2010-Definition of the Criteria of Admissibility of Landfill Waste. *Serie Generale n-281*. 1 December 2010. Available online: <https://www.gazzettaufficiale.it/eli/id/2010/12/01/10A14538/sg> (accessed on 9 April 2022).
42. Gharabaghi, M.; Irannajad, M.; Azadmehr, A. Leaching kinetics of nickel extraction from hazardous waste by sulphuric acid and optimization dissolution conditions. *Chem. Eng. Res. Des.* **2013**, *91*, 325–331. [[CrossRef](#)]
43. Levenspiel, O. *Chemical Reaction Engineering*, 3rd ed.; Wiley: New York, NY, USA, 1998.
44. Souza, A.D.; Pina, P.S.; Lima, E.V.O.; da Silva, C.A.; Leão, V.A. Kinetics of sulphuric acid leaching of a zinc silicate calcine. *Hydrometallurgy* **2007**, *89*, 337–345. [[CrossRef](#)]
45. Lee, I.H.; Wang, Y.J.; Chern, J.M. Extraction kinetics of heavy metal-containing sludge. *J. Hazard. Mater.* **2005**, *123*, 112–119. [[CrossRef](#)]
46. Sakultung, S.; Pruksathorn, K.; Hunsom, M. Simultaneous recovery of valuable metals from spent mobile phone battery by an acid leaching process. *Korean J. Chem. Eng.* **2007**, *24*, 272–277. [[CrossRef](#)]
47. Ho, Y.S.; Harouna-Oumarou, H.A.; Fauduet, H.; Porte, C. Kinetics and model building of leaching of water-soluble compounds of Tilia sapwood. *Sep. Purif. Technol.* **2005**, *45*, 169–173. [[CrossRef](#)]
48. Mbogoro, M.; Snowden, E.; Edwards, M.; Peruffo, M.; Unwin, P. Intrinsic Kinetics of Gypsum and Calcium Sulfate Anhydrite Dissolution: Surface Selective Studies under Hydrodynamic Control and the Effect of Additives. *J. Phys. Chem. C* **2011**, *115*, 10147–10154. [[CrossRef](#)]
49. Jiao, F.; Zhang, L.; Dong, Z.; Namioka, T.; Yamada, N.; Ninomiya, Y. Study on the species of heavy metals in MSW incineration fly ash and their leaching behavior. *Fuel Process. Technol.* **2016**, *152*, 108–115. [[CrossRef](#)]
50. Funatsuki, A.; Takaoka, M.; Oshita, K.; Takeda, N. Methods of determining lead speciation in fly ash by X-ray absorption fine-structure spectroscopy and a sequential extraction procedure. *Anal. Sci.* **2012**, *28*, 481–490. [[CrossRef](#)] [[PubMed](#)]
51. Zhang, Y.; Cetin, B.; Likos, W.J.; Edil, T.B. Impacts of pH on leaching potential of elements from MSW incineration fly ash. *Fuel* **2016**, *184*, 815–825. [[CrossRef](#)]